Global carbon sequestration through continental chemical weathering in a climatic change context

Juan Luis Lechuga-Crespo
Department of Chemical and Environmental Engineering, University of the Basque Country, Plaza Ingeniero Torres Quevedo 1, Bilbao 48013, Basque Country, Spain

Sabine Sauvage
Laboratoire Ecologie Fonctionnelle et Environnement, Université de Toulouse, CNRS, UPS, Toulouse INPT, Campus ENSAT, Avenue de l'Agrobiopole, 31326 Castanet Tolosan CEDEX, France

Michelle vanVliet
Department of Physical Geography, Faculty of Geosciences, Utrecht University, P.O. Box 80115, 3508CB Utrecht, the Netherlands

Estilita Ruiz-Romera
Department of Chemical and Environmental Engineering, University of the Basque Country, Plaza Ingeniero Torres Quevedo 1, Bilbao 48013, Basque Country, Spain

Jean-Luc Probst
Laboratoire Ecologie Fonctionnelle et Environnement, Université de Toulouse, CNRS, UPS, Toulouse INPT, Campus ENSAT, Avenue de l'Agrobiopole, 31326 Castanet Tolosan CEDEX, France

Jose-Miguel Sanchez-Perez (jose-miguel.sanchez-perez@univ-tlse3.fr)
Laboratoire Ecologie Fonctionnelle et Environnement, Université de Toulouse, CNRS, UPS, Toulouse INPT, Campus ENSAT, Avenue de l'Agrobiopole, 31326 Castanet Tolosan CEDEX, France

Research Article

Keywords: hydrology, CO2, river basin, carbon sequestration, hydrology, landscape biogeochemistry

Posted Date: June 15th, 2021

DOI: https://doi.org/10.21203/rs.3.rs-604954/v1

Version of Record: A version of this preprint was published at Scientific Reports on December 1st, 2021. See the published version at https://doi.org/10.1038/s41598-021-02891-y.

Abstract

Here, we simulate carbon dioxide (CO2) sequestration in 300 major world river basins (about 70% of global surface area) through carbonates dissolution and silicate hydrolysis. For each river basin, the daily timescale impacts under both the RCP 2.6 and RCP 8.5 climate scenarios were assessed relative to a historic baseline (1969-1999) using a cascade of models accounting for the hydrological evolution under climate change scenarios. Here we show that global temporal evolution of the CO2 uptake presents a general increase in the annual amount of CO2 consumed from 0.247 Pg C·y-1 to 0.261 and 0.273 Pg C·y-1, respectively for RCP 2.6 and RCP 8.5. Besides, despite showing a general increase for the global daily carbon sequestration, both climate scenarios present a decrease between June and August. Such projected changes have been mapped and evaluated against changes in hydrology, identifying hot spots and moments for the annual and seasonal periods.

Introduction

The chemical weathering of rocks has a significant impact on long-term global climate regulation [1]. It transforms soil CO_2 into inorganic dissolved carbon (such as HCO_3^- and CO_3^{2-}) which is later exported by rivers to other water bodies [2–11]. Riverine dissolved loadings may be used as a proxy for chemical weathering assessment[4,11], and it has been recognised that hydrology impacts these flux-discharge relationships[5-7]. Nevertheless, it is unclear how the potential impacts of climate change will affect these dissolved mass balances. Forecasting how potential short-term (daily or monthly) shifts in hydrology under a changing climate may alter these fluxes of riverine matter is needed to assess potential evolution of the global carbon cycle under a wide range of future scenarios.

In this study, we tested the hypothesis that a greater seasonality of the hydrological cycle would cause a heterogeneous spatial and temporal pattern in CO_2 sequestration at the global scale. We aimed at identifying hot spots and hot moments on which to focus research efforts.

Climate change scenarios forecast increases in atmospheric temperature and an intensification of the hydrological cycle[12]. Still, this augmentation's effect on chemical weathering and related CO_2 uptake dynamics and dissolved solids exportation by rivers is poorly understood[13]. For instance, on one side, an increase in the soil's microbial activity is expected, implying an increase in CO_2 production through respiration[14,15]. However, increasing temperature may decrease CO_2 dissolution in water, as it has been shown that carbonate weathering follows a boomerang-shape evolution with increasing temperature[16]. On the other hand, despite water's widely recognized role as a vector of matter transport and the forecasted changes derived from climate change scenarios[17], the potential implication of these shifts remains misunderstood[13].

How will the annual soil CO_2 consumption evolve under these hydrological shifts? Where and when will these soil CO_2 consumption changes be more relevant? The answer to these scientific questions needs a

large-scale comprehensive study, but such a study is challenging due to the resources needed to be deployed *in situ* to measure the variables involved in these biogeochemical cycles.

In this complex framework, modelling arises as an alternative approach to overcome this challenge by yielding insights into where and when hot spots and hot moments (places and times with disproportionally high chemical weathering rates) may be located. Identifying potential hot spots and moments of change is of interest in deploying resources to understand the mechanistic laws defining them, which could yield relevant insights for landscape biogeochemistry. Two main kinds of models exist: mechanistic if processes are described using a thermodynamic and kinetic base, and empirical when built under parametrical laws derived from historic observational data. Mechanistic models, such as B-WITCH[15,18] and RT-Flux-PIHM[19,20] models, link the thermodynamic, kinetics and transport processes to hydrology and vegetation and have yielded insights, for instance, that 40% of the total increase in CO_2 consumption in the Mackenzie River basin is related to the direct effect of climate change on hydrology alteration[15] or that a “chemostatic” behaviour of riverine dissolved load suggests that hydrological changes impact the dissolved element concentration in rivers[19,20]. Empirical models are commonly developed at large spatial scales[7,21], and their results are used in relevant assessments such as the ESCOBA program[22] and the IPCC Assessment Reports[12].

To accomplish this objective, a cascade of models was set up to cover the 300 largest basins in the world, obtaining the spatial and temporal potential evolution of CO_2 sequestration under two climate change scenarios (RCP 2.6 and RCP 8.5). Both of cations and anions derived from chemical weathering of rocks and associated carbon sequestration were modelled (the reader is referred to the methods section and to the Extended Data Figure 2). Observed data has been used to evaluate the results at each step of the model cascade.

Results And Discussion

Interannual and seasonal fluctuations

The annual mean inorganic C sequestration through chemical weathering during the Historical period (1969–1999) amounts to 0.247 Pg $C{\cdot}y^{-1}$ (1 Pg = 10^{15} g), in the lower range of previous studies[4,8–11,21,23–26], spanning from 0.22 to 0.30 Pg $C{\cdot}y^{-1}$. The climate change scenarios present a potential increase in the amount of C sequestered, reaching mean values of 0.261 and 0.273 Pg $C{\cdot}y^{-1}$ for RCP 2.6 and RCP 8.5, respectively. The annual series (Fig. 1a) shows a similar temporal evolution for the middle part of the century, but such a difference enlarges within the Projection period (2069–2099). An annual average increase in C sequestration of 6% (RCP 2.6) and 10% (RCP 8.5) is forecasted if the Historical period is considered the baseline. The annual increases represent < 0.1% of the anthropogenic emissions projected for the end of the century in the RCP 8.5 scenario, and ~ 0.7% of the "negative emissions" projected for the RCP2.6 scenario[27]. These C sequestration increases are low at the global scale; however, when evaluating the change percentages at a lower time-step (daily), these become more relevant.

When comparing the mean daily temporal evolution in the Projection and the Historical periods (Fig. 1b), more considerable differences are found for the RCP 8.5 scenario. In both scenarios, a positive difference is found for most of the year, agreeing with a more considerable amount of C sequestered during the Projection period compared to the Historical one. Such increases may reach a positive 20% value in May for the RCP 8.5 scenario, followed by a shift towards a decrease between June and August, suggesting a lower CO_2 consumption through continental chemical weathering during these months. Considering that hydrology is the main driver for temporal evolution, a decrease in CO_2 consumption suggests that a lower amount of water is being exported in this period. This decrease coincides with the low discharge period in the northern latitudes, suggesting that these regions have a significant impact on the global amount of soil CO_2 consumed through chemical weathering. Considering that the Northern Hemisphere has a more considerable amount of continental land and that the hydrological cycle is expected to intensify, this could support the insight that the annual shift found between June and August regarding the global carbon weathering CO_2 uptake is a consequence of hydrological changes at these latitudes.

Hot spots and moments for CO_2 uptake

On a global scale, the spatial distribution of carbon sequestration during the Historical period (Fig. 2a) is comparable to what is described in previous literature [7]. Similarly, values are analogous to regional cases, such as the Amazon[11,28,29], Congo[5,21], Niger[30], Garonne[21], the Alps region[31] or the United States continuum[32], even if the river basin's draining lateritic soil covers have lower CO_2 uptake, as shown by Boeglin & Probst[30].

Alterations in this spatial pattern (Fig. 2b) are considered primary consequences of hydrological changes since the geochemical cycles have larger time spans than biogeochemical cycles on the Earth's surface. Larger changes are found in the northern latitudes, where a more significant precipitation, an earlier onset and a more intensive snowmelt in spring[17] are expected to increase the annual discharges in these river basins, even though a higher seasonality will change the hydrological cycle within the year.

A general increasing trend in CO_2 sequestration is found during the January-February-March (JFM) period (**Extended Data** Fig. 1), especially in basins such as the Yenisei and the Ob', which present changes greater than 25%, particularly in the RCP 8.5 scenario. Increasing temperatures are expected to cause an accelerated snowmelt[17], which could explain the increase of dissolved inorganic carbon river fluxes. In contrast, heterogeneous projections are found for southern latitudes, as in the Murray-Darling River basin in Australia and to the Orange River in South Africa. Both these basins are located under mixed climatic zones[33], which could explain the heterogeneous results found in the scenarios. The potential evolution in the river discharge seasonality in these areas may cause different fluxes derived from chemical weathering since a discharge decrease of more than 25% in the low-flow period is expected[17]. However, further analysis using mechanistic approaches or *in situ* measurements is needed to understand and assess potential changes in biogeochemical cycles in these regions during the winter and early spring (JFM) season.

A different pattern is found for the July-August-September (JAS) season, when most of the northern latitudes present negative changes, suggesting a decrease in the CO_2 uptake due to chemical weathering. This shift in the northern latitudes is attributed to a projected decline in discharge, notably on the RCP 8.5 scenario[34].

As discharge intensity is a primary critical factor of CO_2 flux changes in the short-term (daily, monthly or seasonal) assessment, a comparison of the relative changes in CO_2 uptake in a subset of river basins was made for both scenarios (Fig. 3). Such a comparison illustrates how river basins located in tropical and cold climates present large differences for CO_2 uptake, especially river basins in the Siberian region (e.g. Kolima, Khatanga or Lena) or active arc-islands in the Polynesian area (e.g. Fly or Sepik). These changes show that, even with their smaller draining areas and discharges, the role of arc-islands should be taken into consideration and should be a focus of future research as their relative role in carbon sequestration through chemical weathering is relevant [7]. Besides, the potential impacts of climate change in these tropical areas are expected to be more relevant in these smaller river basins than in larger ones like the Amazon or Congo[7].

Similarly, the relative change in CO_2 sequestration on mixed climates' river basins (e.g. the Nile, Krishna, Niger or Murray Darling) is large, which could be related to higher amounts of carbonate rock outcrops in these areas, taking relevant amounts of CO_2 during weathering[35]. Regarding cold and polar basins, permafrost processes were not included in the present analysis, and they are expected to have a significant impact on the carbon sequestration by weathering and the dissolved solid loadings in rivers[36].

Even though there are some relative changes noted at the annual scale, these differences are not maintained throughout the year, neither at the global nor the basin scale. The short-term temporal evolution should be a focus of interest for future research, especially in those areas located in tropical and cold climates, since they seem to be more sensitive to climate change.

Modelling approach limitations

Using a model's output as input to another model, as done in the present study, also implies an accumulation of the error in each step. To assess it, model products have been contrasted with previously published data. The results from the ICWR model show a very significant correlation ($\rho_{SPEARMAN} = 0.83$, $p < 0.01$, $n = 173$, see **Extended Data Fig. 5**) to observed data[26], as well as the MEGA model results in the Historical period[6], ($\rho_{SPEARMAN} = 0.71$, $p < 0.01$, $n = 48$, see **Extended Data Fig. 6**). In summary, even though a cascade of models usually accumulates errors, the present modelling approach fits well with current observed data.

Continental weathering occurs at the critical zone, where slow geological processes interact with faster biogeochemical ones. The present modelling approach includes a macroscale hydrological model which resolves the energy and water balance, the main uncertainties are discussed elsewhere[34]. Concerning the

ICWR model, the parameters have been fitted to observed data for a given situation, these laws may change under a climate change scenario. The MEGA model balance is based in a set of hypotheses described in the literature and summarised in the **Extended Data Fig. 4**. The main limitations of this modelling set up is that it does not simulate transient states, as the chemical weathering rates are described through linear equations. Regolith thickness is kept constant during simulation even though it is coupled to physical erosion which could change chemical weathering rates[37] throughout the simulation. Temporal variation of below-ground CO_2 concentration is not accounted in the ICWR model, even though it has been noted as relevant in silicate weathering and affected by vegetation changes[38].

Conclusion

This study presents a forecast of the potential evolution of CO_2 consumption during the chemical weathering of continental rocks at the global scale under two climate change scenarios. The research provides two main new insights on the temporal evolution of the carbon cycle in the short-term, derived from shifts in the water cycle: a) Even though there is a trend towards increasing the amount of carbon sequestered at the annual and global scale, this pattern is not homogeneously distributed neither in space nor time, and b) the river basins located in cold climates (such as the Kolima, Lena, Yukon, Kuskowin or Yenisey) and in tropical climates with a lower draining area (like the Fly, Sepik or Narmada) may be more sensitive to the effects of climate change.

The insights presented suggest that research on the terrestrial part of the carbon cycle should focus on these areas to constrain the main cycle-shaping drivers better, targeting an understanding of the carbon fluxes' temporal dynamics. This study provides the first snapshot of carbon sequestration's potential evolution through the chemical weathering of rocks on a global scale, which may be used for comparison in future studies in this field.

Methods

Methods and any associated references are available in the online version of the paper.

Declarations

Acknowledgements: Authors wish to thank the Basque Government (Hydro-Environmental Processes Consolidated Group, IT1029-16), the University of the Basque Country (UPV/EHU, UFI11/26), the Institut National Polytechnique de Toulouse (INPT) and the Centre National de la Recherche Scientifique (CNRS) for supporting this research.

Author Contributions: J.L.L.C. contributed by developing the methodology, obtaining the results, and writing the first draft; S.S., E.R.R. and J.M.S.P. assisted in defining the idea; M.T.H.v.V. and J.L.P. discussed the results and contributed to the writing. All authors helped in refining the manuscript.

Additional Information: Extended Data is available in the online version of the paper. Correspondence and requests for materials should be addressed to J.M.S.P. Reprints and permissions information is available at www.nature.com/reprints.

Competing financial interests: The authors declare no competing interests.

Materials & Correspondence: Requests should be made to J.M.S.P.

References

1. Calabrese, S., Parolari, A. J. & Porporato, A. Hydrologic Transport of Dissolved Inorganic Carbon and Its Control on Chemical Weathering. *J. Geophys. Res. Earth Surf.* **122,** 2016–2032; 10.1002/2017JF004346 (2017).

2. Amiotte Suchet, P. & Probst, J. L. Modelling of atmospheric CO2 consumption by chemical weathering of rocks: Application to the Garonne, Congo and Amazon basins. *Chemical Geology* **107,** 205–210; 10.1016/0009-2541(93)90174-H (1993).

3. Amiotte Suchet, P., Probst, J. L. & Ludwig, W. Worldwide distribution of continental rock lithology: Implications for the atmospheric/soil CO2 uptake by continental weathering and alkalinity river transport to the oceans. *Global Biogeochem. Cycles* **17**; 10.1029/2002GB001891 (2003).

4. Bhatt, M. P., Hartmann, J. & Acevedo, M. F. Seasonal variations of biogeochemical matter export along the Langtang-Narayani river system in central Himalaya. *Geochimica et Cosmochimica Acta* **238,** 208–234; 10.1016/j.gca.2018.06.033 (2018).

5. Dupré, B. *et al.* Rivers, chemical weathering and Earth's climate. *Comptes Rendus Geoscience* **335,** 1141–1160; 10.1016/j.crte.2003.09.015 (2003).

6. Gaillardet, J., Dupré, B., Louvat, P. & Allègre, C. J. Global silicate weathering and CO2 consumption rates deduced from the chemistry of large rivers. *Chemical Geology* **159,** 3–30; 10.1016/S0009-2541(99)00031-5 (1999).

7. Hartmann, J., Jansen, N., Dürr, H. H., Kempe, S. & Köhler, P. Global CO2-consumption by chemical weathering: What is the contribution of highly active weathering regions? *Global and Planetary Change* **69,** 185–194; 10.1016/j.gloplacha.2009.07.007 (2009).

8. Probst, J. L., Ludwig, W. & Amiotte Suchet, P. Global modeling of CO2 uptake by continental erosion and of carbon river transport to the oceans. / Modélisation à l'échelle globale des flux de CO2 consommé par l'érosion continentale et des transports fluviaux de carbone vers les océans. *sgeol* **50,** 131–156; 10.3406/sgeol.1997.1950 (1997).

9. Probst, J. L., Mortatti, J. & Tardy, Y. Carbon river fluxes and weathering CO2 consumption in the Congo and Amazon river basins. *Applied Geochemistry* **9,** 1–13; 10.1016/0883-2927(94)90047-7 (1994).

10. Dessert, C., Dupré, B., Gaillardet, J., François, L. M. & Allègre, C. J. Basalt weathering laws and the impact of basalt weathering on the global carbon cycle. *Chemical Geology* **202,** 257–273; 10.1016/j.chemgeo.2002.10.001 (2003).

11. Oliva, P., Villa, I. M. & Dupré, B. Chemical weathering in granitic environments. *Chemical Geology* **202,** 225–256; 10.1016/j.chemgeo.2002.08.001 (2003).

12. Ciais, P. *et al.* Carbon and other biogeochemical cycles. In *Climate Change 2013: The Physical Science Basis. Contribution of Working Group I to the Fifth Assessment Report of the Intergovernmental Panel on Climate Change,* edited by T. F. Stocker*, et al.* (Cambridge, New York, 2013).

13. Liu, Z., Dreybrodt, W. & Wang, H. A new direction in effective accounting for the atmospheric CO2 budget: Considering the combined action of carbonate dissolution, the global water cycle and photosynthetic uptake of DIC by aquatic organisms. *Earth-Science Reviews* **99,** 162–172; 10.1016/j.earscirev.2010.03.001 (2010).

14. Beaulieu, E., Goddéris, Y., Donnadieu, Y., Labat, D. & Roelandt, C. High sensitivity of the continental-weathering carbon dioxide sink to future climate change. *Nature Clim Change* **2,** 346–349; 10.1038/nclimate1419 (2012).

15. Conant, R. T. *et al.* Temperature and soil organic matter decomposition rates - synthesis of current knowledge and a way forward. *Glob. Change Biol.* **17,** 3392–3404; 10.1111/j.1365-2486.2011.02496.x (2011).

16. Gaillardet, J., Calmels, D., Romero-Mujalli, G., Zakharova, E. & Hartmann, J. Global climate control on carbonate weathering intensity. *Chemical Geology* **527,** 118762; 10.1016/j.chemgeo.2018.05.009 (2019).

17. van Vliet, M. T. H. *et al.* Global river discharge and water temperature under climate change. *Global Environmental Change* **23,** 450–464; 10.1016/j.gloenvcha.2012.11.002 (2013).

18. Roelandt, C., Goddéris, Y., Bonnet, M.-P. & Sondag, F. Coupled modeling of biospheric and chemical weathering processes at the continental scale. *Global Biogeochem. Cycles* **24**; 10.1029/2008GB003420 (2010).

19. Bao, C., Li, L., Shi, Y. & Duffy, C. Understanding watershed hydrogeochemistry: 1. Development of RT-Flux-PIHM. *Water Resour. Res.* **53,** 2328–2345; 10.1002/2016WR018934 (2017).

20. Li, L. *et al.* Expanding the role of reactive transport models in critical zone processes. *Earth-Science Reviews* **165,** 280–301; 10.1016/j.earscirev.2016.09.001 (2017).

21. Amiotte Suchet, P. & Probst, J. L. A global model for present-day atmospheric/soil CO2 consumption by chemical erosion of continental rocks (GEM-CO2). *Tellus B* **47B,** 273–280; 10.1034/j.1600-0889.47.issue1.23.x (1995).

22. Aumont, O. *et al.* Riverine-driven interhemispheric transport of carbon. *Global Biogeochem. Cycles* **15,** 393–405; 10.1029/1999GB001238 (2001).

23. Berner, R. A., Lasaga, A. C. & Garrels, R. M. The carbonate-silicate geochemical cycle and its effect on atmospheric carbon dioxide over the past 100 million years. *American Journal of Science* **283,** 641–683; 10.2475/ajs.283.7.641 (1983).

24. Meybeck, M. Global chemical weathering of surficial rocks estimated from river dissolved loads. *American Journal of Science* **287,** 401–428; 10.2475/ajs.287.5.401 (1987).

25. Munhoven, G. Glacial-interglacial changes of continental weathering: estimates of the related CO2 and HCO3 flux variations and their uncertainties. *Global and Planetary Change* **33,** 155–176; 10.1016/S0921-8181(02)00068-1 (2002).

26. Probst, J. L. Géochimie et hydrologie de l'érosion continentale. Mécanismes, bilan global actuel et fluctuations au cours des 500 derniers millions d'années. Université Louis-Pasteur, 1992.

27. van Vuuren, D. P. *et al.* The representative concentration pathways: an overview. *Climatic Change* **109,** 5–31; 10.1007/s10584-011-0148-z (2011).

28. Moquet, J.-S. *et al.* Amazon River dissolved load: temporal dynamics and annual budget from the Andes to the ocean. *Environmental science and pollution research international* **23,** 11405–11429; 10.1007/s11356-015-5503-6 (2016).

29. Mortatti, J. & Probst, J.-L. Silicate rock weathering and atmospheric/soil CO2 uptake in the Amazon basin estimated from river water geochemistry: seasonal and spatial variations. *Chemical Geology* **197,** 177–196; 10.1016/S0009-2541(02)00349-2 (2003).

30. Boeglin, J. L. & Probst, J. L. Physical and chemical weathering rates and CO2 consumption in a tropical lateritic environment: the upper Niger basin. *Chemical Geology* **148**; 10.1016/S0009-2541(98)00025-4 (1998).

31. Donnini, M. *et al.* Chemical weathering and consumption of atmospheric carbon dioxide in the Alpine region. *Global and Planetary Change* **136,** 65–81; 10.1016/j.gloplacha.2015.10.017 (2016).

32. Moosdorf, N., Hartmann, J., Lauerwald, R., Hagedorn, B. & Kempe, S. Atmospheric CO2 consumption by chemical weathering in North America. *Geochimica et Cosmochimica Acta* **75,** 7829–7854; 10.1016/j.gca.2011.10.007 (2011).

33. Beck, H. E. *et al.* Present and future Köppen-Geiger climate classification maps at 1-km resolution. *Scientific data* **5,** 180214; 10.1038/sdata.2018.214 (2018).

34. van Vliet, M. T. H., Wiberg, D., Leduc, S. & Riahi, K. Power-generation system vulnerability and adaptation to changes in climate and water resources. *Nature Clim Change* **6,** 375–380;

10.1038/NCLIMATE2903 (2016).

35. Amiotte Suchet, P. & Probst, J. L. Origines du carbone inorganique dissous dans les eaux de la Garonne. Variations saisonnières et interannuelles. / Sources of dissolved inorganic carbon in the Garonne river water. Seasonal and inter annual variations. *sgeol* **49,** 101–126; 10.3406/sgeol.1996.1938 (1996).

36. Streletskiy, D., Anisimov, O. & Vasiliev, A. Permafrost Degradation, 303–344; 10.1016/B978-0-12-394849-6.00010-X (2015).

37. Millot, R., Gaillardet, J., Dupré, B. & Allègre, C. J. The global control of silicate weathering rates and the coupling with physical erosion: new insights from rivers of the Canadian Shield. *Earth and Planetary Science Letters* **196,** 83–98; 10.1016/S0012-821X(01)00599-4 (2002).

38. Beaulieu, E. *et al.* Impact of atmospheric CO 2 levels on continental silicate weathering. *Geochem. Geophys. Geosyst.* **11**; 10.1029/2010GC003078 (2010).

Methods

Four Representative Concentration Pathways (RCP) were selected by the Intergovernmental Panel on Climate Change (IPCC) in its fifth Assessment Report[12] regarding climate change impacts on the carbon cycle. Of those four RCPs, two are included in the present analysis (RCP 2.6 and RCP 8.5) under two assumptions. RCP 2.6 considers that the radiative forcing (i.e. the strength of change drivers) will peak in 2100 at about 2.6 $W{\cdot}m^{-2}$ and then decline, whereas RCP 8.5 considers that the radiative forcing will reach >8.5 $W{\cdot}m^{-2}$ by 2100. The highest and lowest RCPs were selected to capture the broadest range of uncertainties in atmospheric greenhouse gas concentrations. Bias-corrected climate model outputs of five general circulation models were included in the VIC hydrological model to simulate impacts on daily river discharge on 0.5°x0.5° at the global scale[34]: GFDL-ESM2M[39,40], the HadGEM2-ES[41,42], the IPSL-CM5A-LR[43], the MIROC-ESM-CHEM[44], and the NorESM1-M[45]. Validation results showed that the observed hydrological conditions were realistically represented by the VIC hydrological model for most river basins.

The present study's input data handling and modelling follows the workflow summarized in **Extended Data Figure 2**. First, a subset of the 300 largest river basins covering ~70% of global land area was selected from the HydroBASINS dataset[46], including only exorheic river basins (**Extended Data Figure 3**). The catchment area selected was derived from the HydroBASINS dataset. Second, the outlet points of river basins from the simulated river discharge VIC database were selected manually by exploring the time series for each sampling location and the surrounding points (±0.5°) to choose the correct outlet. When a catchment presented several outlets (which is common for endorheic catchments draining to a lake or inner sea), all of them were considered, and their discharge was added to account for all water flowing out of the drainage surface. Deconvolution of the daily discharge signal for each outlet is applied to distinguish between the surface runoff from the soil and groundwater flow. Third, draining area

characteristics are summarized for each river basin by considering the relative abundance of lithological classes contained in the Global Lithological Map[47] (GLIM), the soil classes as defined by the Harmonized World Soil Database[48] (HWSD), and the climatic zones present according to the Köppen-Geiger classification presented by Beck et al.[33]. The modelling approach consists of two models in cascade; the flux of ions derived from the chemical weathering of rocks is computed using the ICWR[49] model daily for each river basin under each discharge time series. Then, the Major Element Geochemical Approach[35] (MEGA) model uses these loadings to estimate the CO_2 consumed through chemical weathering.

From this set-up, a daily time series of major ion river fluxes and CO_2 consumption through chemical weathering from the 300 largest river basins was obtained from 1965 to 2100. Two periods are established to estimate the potential effect of hydrological shifts on weathering CO_2 consumption: the Historical (October 1969-September 1999) and the Projection (October 2069-September 2099). A comparison between the two periods is also accomplished. Daily discharge time series have been taken from all these scenario-model combinations while temporal aggregation is performed after applying the ICWR and MEGA models.

The stream discharge time series have been deconvoluted to separate the influence of the diluted surface runoff from the baseflow and interflow discharges. Such deconvolution is performed following the digital filter shown in **Equation 1**, as proposed by Eckhardt[50]. In the present study, only interflow and baseflow are considered significantly loaded with ions, while surface runoff is the main agent for dilution. A digital filter based on the slopes of the increasing and decreasing parts of the hydrograph was selected. It is sensitive not only to changes in the amount of water but also to seasonality and flood events. Nonetheless, this is a source of uncertainty as the infiltration process depends on catchment-to-catchment properties, while this equation assumes linearity between the groundwater outflow (baseflow) and its storage[50].

$$b(t) = \frac{(1-BFI_{mx})\cdot a\cdot b(t-1)+(1-a)\cdot BFI_{mx}\cdot Q(t)}{1-a\cdot BFI_{mx}},\ \text{for } b(t) < Q(t) \quad \textbf{Equation 1}$$

Where *b(t)* is the baseflow time series, BFI_{mx} represents the long-term ratio of baseflow to total streamflow, *a* is the filter parameter, and *Q(t)* is the total discharge. When *b(t)>Q(t)*, then *b(t)* is replaced by *Q(t)*. The parameters that were selected for the separation were $BFI_{mx} = 0.8$ and $a = 0.95$ (as recommended by Xie et al.[51]). These parameters were kept constant in all catchments, which also become a source of uncertainty.

The ICWR model is an empirical model that was developed to estimate major ion riverine fluxes released by chemical weathering of rocks at the global scale, based on **Equation 2**, and it has been validated at the global scale under static conditions[49] and at the local scale under dynamic evolution[52]. Computing it requires a description of the draining area of each river basin in terms of soil coverture and lithological distribution. The parameters of the equation take into account the concentration for each ion *x* drained

from a lithological class *i*. The ICWR model parameters were calibrated after an atmospheric input correction, thus the loadings computed from this equation only relate to the chemical weathering process, which are needed input for the MEGA model.

$F_x(t) = b(t) \cdot f_{sx} \cdot \sum(L_i \cdot C_{ix})$ **Equation 2**

Where F_x represents the specific flux of ion *x* in mol·km^{-2}·y^{-1}, *b* represents the baseflow and interflow obtained from the deconvolution of the total discharge signal, f_{sx} is a factor considering the soil shielding effect on CW (adim), L_i is the relative abundance of a lithological class *i* in terms of the total area of the drainage basin (expressed in the 0-1 range), and C_{ix} is the calibrated parameter that represents the concentration of the ion *x* draining from the lithological class (expressed in mol·L^{-1}). This equation is applied to the time series of the deconvoluted discharge, including the baseflow and interflow.

The MEGA model is based on the mass balance showed in **Extended data Figure 4**[35]. The input data are the riverine molar loadings of each major ion, after the atmospheric input correction and under the assumption that anthropogenic influence is not captured in the measurements of major ion concentrations, as well as the R_{pyr} and R_{sil} molar ratios for each catchment, which account for the Ca^{2+}+Mg^{2+} loads coming from the weathering of silicate rocks and the SO_4^{2-} originating from pyrite oxidation, respectively. The results from this model relate to the CO_2 consumed by the CW of rocks.

Considering the river loadings of all major ions, the CO_2 consumed is computed as follows: first, the atmospheric deposition (wet and dry) must be removed from these loads, remaining the molar fluxes derived from CW. All Cl^- is associated with the dissolution of halite (NaCl), though remaining Na^+ is associated with Na-silicates. If the Cl^->Na^+, the remaining Cl^- is linked to the dissolution of sylvite (KCl). Evaporites do not uptake any CO_2 when dissolving, while Na^+ and K^- silicate rocks (e.g. albite $NaAl_3O_8$ and orthoses $KAlSi_3O_8$) require 1 mol CO_2 for each ion mol released to water. Then, using R_{pyr}, it is possible to discriminate the SO_4^{2-} load released respectively by gypsum ($CaSO_4$) dissolution and pyrite (FeS_2) oxidation. Gypsum does not consume any CO_2 during dissolution, while pyrite releases 2 mol CO_2 for each SO_4^{2-} ion released. Later, the C_b (molar flux of Ca^{2+} and Mg^{2+} released by carbonates dissolution) is computed using R_{sil} to account for how much Ca^{2+} and Mg^{2+} derived from the weathering of the carbonates; a 60% of Ca^{2+} is linked to calcite ($CaCO_3$) dissolution while the remaining 40% is released by dolomite ($CaMgCO_3$) dissolution. The dissolution of calcite and dolomite also takes up 1 mol of CO_2. The remaining Ca^{2+} and Mg^{2+} fluxes are linked to silicates which consume 2 mol CO_2. A further description of the model calculation is found in Amiotte-Suchet[53], Amiotte Suchet and Probst[35] and Donnini et al.[31]. The R_{pyr} and R_{sil} values used in the present study are compiled in the **Extended Data Table 1**.

Two 30-year periods are considered in the present study: a Historical (1969-1999) and a Projection (2069-2099), both computed at the daily time scale. The potential impacts derived from climate change are

computed by quantifying the relative difference in the Projection period to the Historical period, following **Equation 3**. Where ΔCO_2 denotes the relative change for each basin (expressed in %), and L_{CO2} represents the mean amount of CO_2 consumed through CW of rocks, during the Projection and Historical period, expressed in Mg C·y^{-1}. This result analysis is divided into two steps: at the annual scale, where L_{CO2} is the mean annual amount of CO_2 consumed in each period; and at the season scale, where L_{CO2} symbolizes the mean amount of CO_2 consumed during all the springs, summers, autumns, and winters of each period.

$$\Delta CO_2(\%) = \frac{\left(L_{CO_2}^{Projection} - L_{CO_2}^{Historical}\right)}{L_{CO_2}^{Historical}} \cdot 100 \qquad \textbf{Equation 3}$$

Data availability

The data that support the findings of this study are available from the corresponding author upon reasonable request.

METHODS REFERENCES

39. Delworth, T. L. *et al.* GFDL's CM2 Global coupled climate models. Part I: Formulation and Simulation Characteristics. *American Meteorological Society* **19,** 643–674; 10.1175/JCLI3629.1 (2006).

40. Donner, L. J. *et al.* The Dynamical Core, Physical Parameterizations, and Basic Simulation Characteristics of the Atmospheric Component AM3 of the GFDL Global Coupled Model CM3. *Journal of Climate* **24,** 3484–3519; 10.1175/2011JCLI3955.1 (2011).

41. Collins, W. J. *et al.* Development and evaluation of an Earth-system model – HadGEM2. *Geosci. Model Dev. Discuss.* **4,** 997–1062; 10.5194/gmdd-4-997-2011 (2011).

42. Martin, G. M. *et al.* The HadGEM2 family of Met Office Unified Model climate configurations. *Geoscientific Model Development* **4,** 723–757; 10.5194/gmd-4-723-2011 (2011).

43. Dufresne, J.-L. *et al.* Climate change projections using the IPSL-CM5 Earth System Model: from CMIP3 to CMIP5. *Clim Dyn* **40,** 2123–2165; 10.1007/s00382-012-1636-1 (2013).

44. Watanabe, S. *et al.* MIROC-ESM 2010: model description and basic results of CMIP5-20c3m experiments. *Geosci. Model Dev.* **4,** 845–872; 10.5194/gmd-4-845-2011 (2011).

45. Iversen, T. *et al. The Norwegian Earth System Model, NorESM1-M-Part 2: Climate response and scenario projections, Geosci. Model Dev., 6, 389-415* (2013).

46. Lehner, B. & Grill, G. *Global river hydrography and network routing: baseline data and new approaches to study the world's large river systems*. *Hydrol. Process.*, 27, 2171–2186. Available at www.hydrosheds.org (2013).

47. Hartmann, J. & Moosdorf, N. The new global lithological map database GLiM: A representation of rock properties at the Earth surface. *Geochem. Geophys. Geosyst.* **13**; 10.1029/2012GC004370 (2012).

48. FAO, IIASA, ISRIC, ISS-CAS & JRC. Harmonized World Soil Database (version 1.2). FAO, 2012.

49. Lechuga-Crespo, J. L. *et al.* A model to evaluate chemical weathering from riverine transports of dissolved major elements at global scale. *Global and Planetary Change* **192**; 10.1016/j.gloplacha.2020.103226 (2020).

50. Eckhardt, K. How to construct recursive digital filters for baseflow separation. *Hydrol. Process.* **19,** 507–515; 10.1002/hyp.5675 (2005).

51. Xie, J. *et al.* Evaluation of typical methods for baseflow separation in the contiguous United States. *Journal of Hydrology* **583,** 124628; 10.1016/j.jhydrol.2020.124628 (2020).

52. Lechuga-Crespo, J. L., Sauvage, S., Ruiz-Romera, E., George, C. & Sánchez-Pérez, J. M. SWATLitho: A hydrogeochemical model to estimate daily geochemical loads at the catchment scale. *Environmental Modelling & Software* **135,** 104893; 10.1016/j.envsoft.2020.104893 (2021).

53. Amiotte Suchet, P. Cycle du carbone, érosion chimique des continents et transferts vers les océans. Université Louis-Pasteur, 1995.

Extended Data Table

Extended Data Table 1. R_{sil} and R_{pyr} molar ratios calculated for each lithological class and compared with Amiotte Suchet and Probst[35]. R_{pyr}* relates to the actual values selected, due to the worse representation of the SO_4^{2-} in the ICWR model, these are taken from Amiotte Suchet and Probst[35].

Rock types	Source	R_{sil}	R_{pyr}	R_{pyr}*
Plutonic and metamorphics	Amiotte Suchet and Probst[35]	1,50	0,15	
Volcanic acid		1,20	0,02	
Basalt		0,50	0,02	
Sand and sandstones		1,30	0,24	
Clay detrital rocks (Shales)		0,50	0,19	
Evaporitic	Lechuga-Crespo et al.[49]			
Metamorphics		0,23	0,26	0,15
Plutonic Acid		0,97	0,00	0,15
Plutonic Basic		4,67	0,00	0,15
Plutonic Intermediate		3,06	0,08	0,15
Pyroclastics		1,16	0,07	0,02
Sedimentary carbonates				
Sedimentary mixed		0,35	0,34	0,19
Sedimentary siliciclastics		1,13	0,13	0,24
Sedimentary unconsolidated		1,10	0,11	0,24
Volcanic acid		1,26	0,17	0,02
Volcanic basic		0,40	0,30	0,02
Volcanic intermediate		0,25	0,48	0,02

R_{pyr} ($mol \cdot mol^{-1}$)= $SO_4^{2-}/(Na^+ + K^+ + Ca^{2+} + Mg^{2+})$ and R_{sil} ($mol \cdot mol^{-1}$)= $(Na^+ + K^+)/(Ca^{2+} + Mg^{2+})$ for water draining silicate rocks. R_{pyr}* are taken from Amiotte Suchet and Probst[35] considering the minerals corresponding to each lithological group[47].

Figures

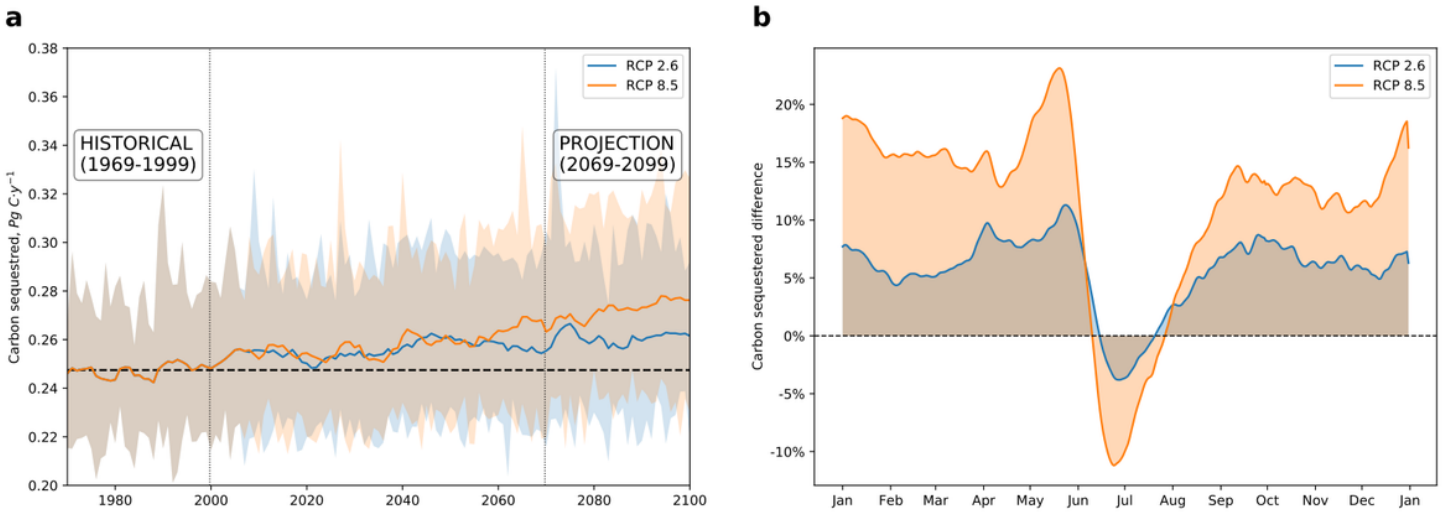

Figure 1

Temporal evolution of the global soil CO2 sequestered for the RCP 2.6 (blue) and RCP 8.5 (orange) scenario: a) interannual fluctuations in annual weathering CO2 consumption, where shaded areas represent the minimum and maximum amount of annual carbon sequestered in five general circulation models, and the solid lines account for a 10-year moving average to evaluate the pattern. The dashed horizontal line represents the mean consumption for the Historical period. b) Seasonal variations for the daily mean relative difference between the Projection and Historical periods.

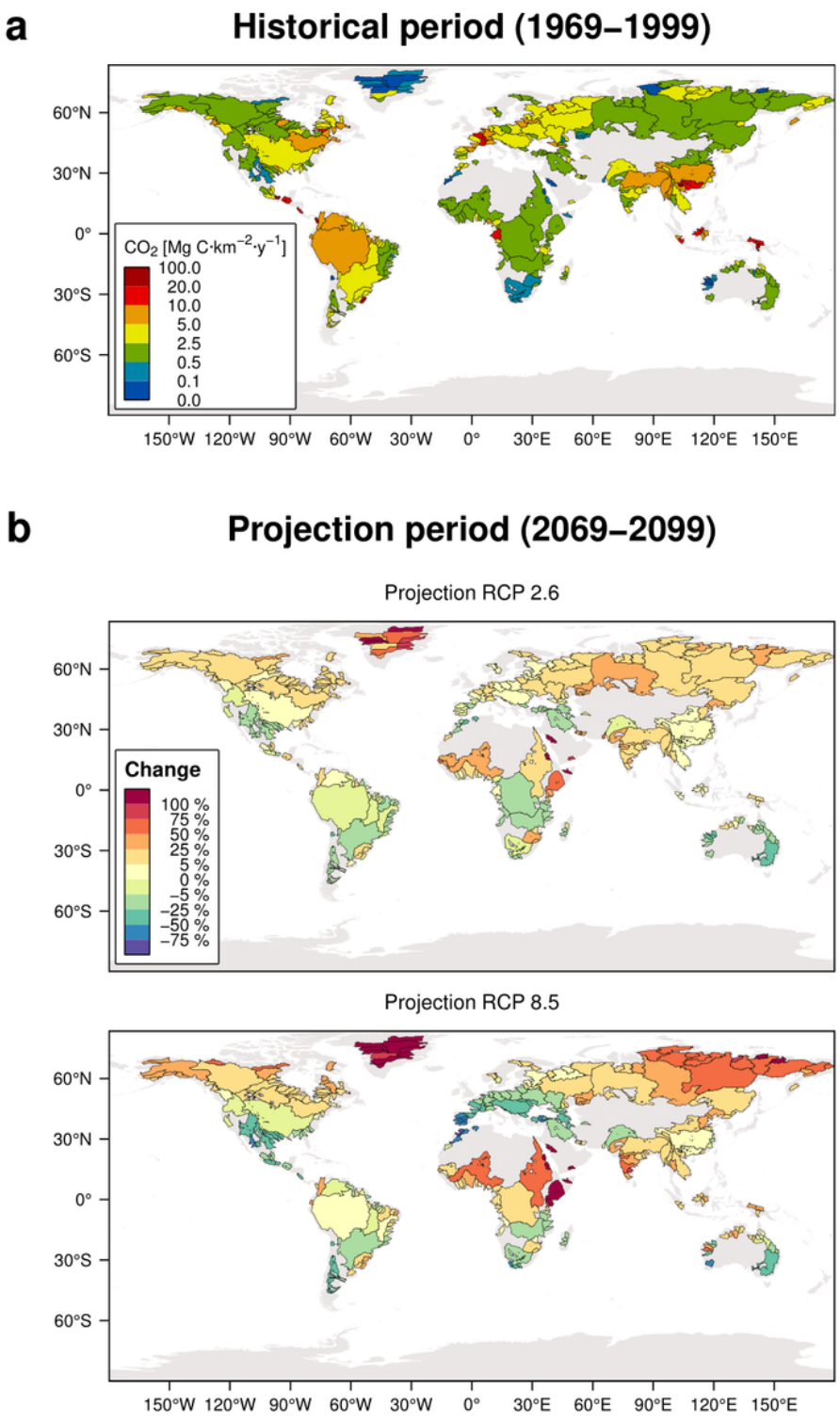

Figure 2

a) Interannual mean CO2 consumption through chemical weathering during the Historical period, expressed as Mg C·y-1·km-2; and b) relative change for the Projection period in the RCP 2.6 and RCP 8.5 climate scenarios, expressed as a percentage of change regarding the Historical period. Note: The designations employed and the presentation of the material on this map do not imply the expression of any opinion whatsoever on the part of Research Square concerning the legal status of any country,

territory, city or area o bbnhjr of its authorities, or concerning the delimitation of its frontiers or boundaries. This map has been provided by the authors.

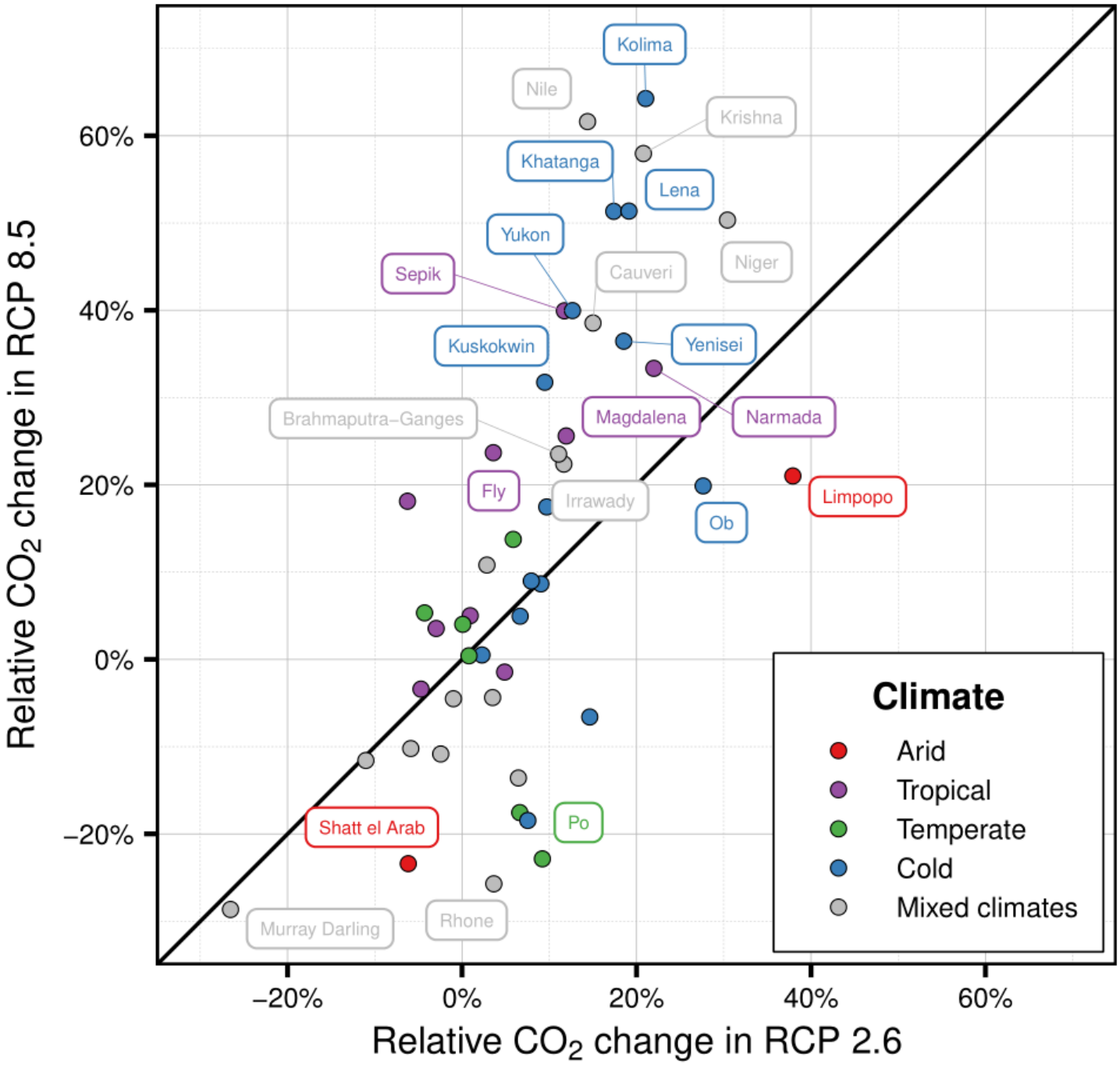

Figure 3

Comparison of the relative CO2 uptake change in the river basins used for MEGA21 model validation for both climatic scenarios. Only river basins showing a relative change over ±20% are labelled. The straight black line represents equal change.

Supplementary Files

This is a list of supplementary files associated with this preprint. Click to download.

- ExtendedDataFigure1.png
- ExtendedDataFigure2.png
- ExtendedDataFigure3.png
- ExtendedDataFigure4.png
- ExtendedDataFigure5.png
- ExtendedDataFigure6.png